

# Mechanical behavior of a floating model pile in unsaturated expansive soil associated with water infiltration

Dr. NIRMAL KUMAR SAHOO

Associate Professor, Dept. of Civil Engineering, Aryan Institute of Engineering & Technology, Bhubaneswar

KAMALAKANTA SEN

Professor, Department of Civil Engineering, Raajdhani Engineering College, Bhubaneswar, Odisha

---

## Abstract

Pile foundations are widely designed extending principles of saturated soil mechanics assuming drained conditions (i.e. effective stress) even in expansive soil deposits despite the fact the soil around the pile is in a state of unsaturated condition. The mechanical behavior of in-situ pile foundations are significantly influenced by suction changes associated with water infiltration. In this paper, a single model pile mechanical behavior variations associated with suction changes in an unsaturated expansive soil under a service load were investigated. Experimental results suggest pile settlement increases due to water infiltration. Such a phenomenon can be attributed to pile shaft friction reduction in the active zone associated with suction reduction due to water infiltration and volume expansion of the soil. Experimental results were also simulated and interpreted using a computation program, PEI (i.e. Pile behavior in Expansive soil upon Infiltration), which was proposed based on principles of unsaturated soil mechanics. A theoretical model was proposed for the estimation of threshold pile head load which distinguishes whether the pile would experience upward or downward movement upon water infiltration. The theoretical model and the numerical modeling approach presented in this are valuable for practicing engineers in the rational design of piles taking account of the mechanical behavior of expansive soils.

---

## 1. Introduction

Ground heave or settlement induced by seasonal wetting and drying conditions contribute to severe distress to various civil infrastructures constructed in expansive soils (Phanikumar et al. 2004; Sharma and Phanikumar 2005; Yitagesu et al. 2009; Jaremski 2012; Liu and Vanapalli 2017; Jiang et al. 2018; Jain and Jha 2020). Studies by Adem and Vanapalli (2016) highlight the steadily increasing economic losses associated with expansive soils during the past five decades all over the world. Piles are most preferred foundations for infrastructure constructed on or in

expansive soils (Poulos and Davis 1980; Al-Rawas and Goosen 2006; Nelson et al. 2012). End bearing pile foundations in expansive soils can effectively transfer the loads from superstructure to a deeper stable soil stratum or bed-rock to provide adequate bearing capacity. Due to this reason, steel and concrete piles have been widely used in engineering practice in Sudan since 1970s (Elsharief 1987; Nur Eldayem 1999; Mohamedzein et al 1999), where expansive soils cover about 40% of the total area (Osman and Charlie 1983). In addition, floating piles or under reamed piles are also used without depending on end

resistance when a stable stratum is not available at a shallow depth (Mohamedzein et al. 1999; Osman and Elsharief 1999; Prakash and Ramakrishna 2004; Al-Rawas and Goosen 2006; Sheng et al. 2008). Floating piles are uniform diameter slender columns; however, under reamed piles are columns with one or more bulbs at specified locations along their depths that are typically constructed using reinforced concrete. Under reamed piles offer more resistance to vertical compressive and uplift loads (Prakash and Ramakrishna 2004). The conventional, floating and under reamed piles are widely used in various countries which include Australia, Canada, China and India, where expansive soils are widely distributed.

For piles in unsaturated expansive soils with high suction values, water infiltration influences the mechanical behavior of soil around the pile in three different ways. Firstly, suction of the soil around the pile reduces significantly. Secondly, volume expansion triggers ground heave in the vertical direction. Thirdly, in the horizontal direction, volume expansion restriction by the pile contributes to lateral swelling pressure mobilization which adds an additional increment to the lateral earth pressure due to soil self-weight and surcharge. All these changes contribute to variations in the load transfer mechanisms of piles in unsaturated expansive soils.

Various model and in-situ test results summarized in the literature provide valuable information related to the mechanical behavior variations of pile foundations in expansive soils upon water infiltration (Fan et al. 2007; Wu et al. 2012; Mendoza 2013; Yang et al. 2017; Soundara and Robinson 2017). However, most experimental investigations focus has been directed to understand the uplift movement of the pile and/or the uplift force generated during the infiltration process. Studies that provide detailed description related to the pile load transfer mechanism such as the pile shaft friction distribution is quite limited. Furthermore, there are limited studies that focus on pile foundations behavior which consider the influence of matric suction, which is a stress state variable that influences the mechanical behavior of unsaturated soils coupled with net normal stress (Lu 2008). This may be attributed to the difficulties associated with the real time measurement of soil suction. In other words, comprehensive understanding of mechanical behavior of floating piles in expansive soils is presently lacking in the literature.

In this study, considering a most unfavorable scenario, a floating model Pile Infiltration Test (PIT) was specially designed and performed in the University of Ottawa geotechnical engineering laboratory. The typically encountered stress and hydraulic boundary conditions during the service stage of the pile were applied while performing the PIT. Real-time measurement on pile mechanical behaviors (including the pile axial force distribution and pile head displacement) and soil properties/behaviors (including soil displacement, water content and suction) were determined

to rigorously interpret the pile mechanical behavior variations during the entire testing process. Comparisons were

The free swell index is tested according to IS 2720, which is calculated according to following equations:  $I_f = [(V_d - V_k) / V_k] \times 100\%$ .

provided between the measured experimental data and simulations using a program PEI (Pile behavior in Expansive soil upon Infiltration) proposed by Liu and Vanapalli (2019a), which is based on unsaturated soil mechanics. In addition, a theoretical model is proposed for the estimation of threshold pile head load, which provides information whether the pile would experience an upward or downward movement upon water infiltration. Theoretical analyses along with the experimental and modeling results summarized in this paper are useful for practicing engineers in the rational design of floating pile foundations in expansive soils.

## 2. Model pile infiltration test (PIT) performed in Regina clay

### 2.1. Soil physical and mechanical properties tests

The physical soil properties of Regina clay determined following ASTM standards are summarized in Table 1. From the information gathered from the compaction curve, experimental investigations were decided to be performed at a gravimetric water content of 27% (which is dry side optimum moisture content) and a dry density of 1367 kg/m<sup>3</sup>. The purpose of setting the initial water content less than the optimum water content of 29% is to enable a more significant swelling pressure and volume expansion to be mobilized. Identical soil samples with the same water content and dry density were used in both SWCC measurement and PIT. However, the interface shear strength tests were performed on soil samples prepared at different initial compaction water contents but at the same soil dry density (i.e. 1367 kg/m<sup>3</sup>). More details of the interface shear strength tests are discussed in a later section.

Fig. 1 summarizes the SWCC of Regina clay measured considering volume changes of soil specimen. The SWCC is plotted as a relationship between gravimetric water content versus suction, volumetric water content versus suction and degree of saturation versus suction. It should be noted that the SWCC measured and used in the analysis of the model PIT was under zero stress boundary condition. This is considered to be reasonable since in the PIT, the model pile is placed in expansive soil layer which is only 0.4 m

Table 1  
Physical and mechanical properties of Regina clay.

Liquid limit, LL (%)	89
Plastic limit, PL (%)	32
Plastic index, PI	57
Specific gravity, G	2.85
Maximum dry density, $q_{d,max}$ (kg/m <sup>3</sup> )	1382
Optimum water content, w (%)	29
Vertical swelling pressure, $P_s$ , (kPa)	136
Free swell index, $I_f$ (%)	100.6

Note: The vertical swelling pressure is tested under constant volume condition from a gravimetric water content of 27% to fully saturation;

thickness; the influence of vertical stress on the soil volume change associated with this thickness can be assumed negligible. Furthermore, the SWCC behavior is essentially hysteretic; due to this reason, for a certain suction value, the water content associated with wetting path is less than that for a drying path (Pham et al. 2005). However, the measurement of a complete set of hysteretic SWCCs is time-consuming and costly. In addition, it is difficult to represent these curves in a simple mathematical form for use in routine engineering practice (Fredlund 2019). For these reasons, in the present study, the SWCC is assumed non-hysteretic in nature for simplicity purposes (Pham et al. 2005).

The peak shear strength of saturated soil and saturated interface can be described by Mohr-Coulomb failure criteria, which are shown as Eq. (1) and (2), respectively. Eq. (3) proposed by Fredlund et al. (1978) expressed in terms of two independent stress state variables; namely, net normal stress and matric suction is commonly used to model the peak shear strength of unsaturated soil (e.g., Oloo and Fredlund 1996; Vanapalli et al. 1996). Hamid and Miller (2009) suggested that the shear strength of the soil-structure interface can be interpreted using Eq. (4) which is similar to Eq. (3).

where  $r_{nf}$  is the normal stress on the failure plane at failure;  $u_{af}$  is the pore air pressure on the failure plane at failure;  $u_{wf}$  is the pore water pressure on the failure plane at failure;  $(r_{nf} - u_{af})$  is the net normal stress on the failure plane at failure; and  $(u_{af} - u_{wf})$  is the matric suction on the failure plane at failure;  $l'$  is the internal friction angle with respect to net normal stress;  $l^b$  is the angle of friction with respect to matric suction;  $d'$  is the interface friction angle with respect to net normal stress;  $d^b$  is the interface friction angle with respect to matric suction;  $c'$  is the cohesion;  $c'_a$  is the interface cohesion.

Various shear strength parameters in Eq. (1) to (4) were determined through a series of soil and interface direct shear tests under both saturated and unsaturated conditions. For interface shear tests, a prefabricated aluminum block was used to simulate the pile surface by pasting a thin layer of fine sand using epoxy and placed at the shear chamber bottom. Compacted soil specimens were prepared at the same dry density ( $1367 \text{ kg/m}^3$ ) but with different water content values of 24%, 27% and 30%, which correspond to different suction values. Three different vertical

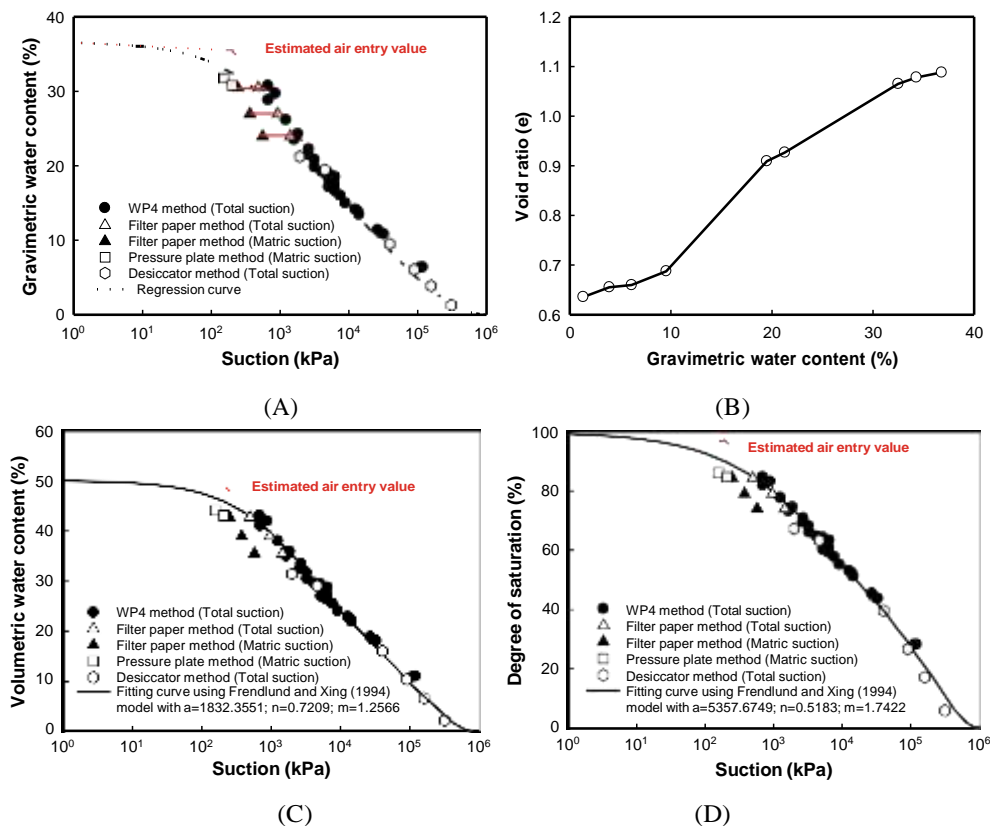


Fig. 1. SWCC of Regina clay measured over the entire suction range (A) Variation of gravimetric water content with respect to soil suction; (B) Variation of void ratio with respect to the gravimetric water content; (C) Variation of volumetric water content with respect to soil suction; (D) Variation of degree of saturation with respect to soil suction. (See above-mentioned references for further information.)

Cohesion ( $c'$ )	14 kPa
Interface cohesion ( $c'_a$ )	8 kPa

stresses, namely 50 kPa, 100 kPa and 150 kPa were applied. Saturated soil and interface shear tests were conducted under consolidated drained conditions. The shear chamber was sealed to ensure the shear tests were conducted under constant water content conditions for performing unsaturated shear tests. Under constant water content conditions, the soil water menisci that forms during the compaction process would still be in a relative intact state and contribute to the peak shear strength (i.e. for unsaturated soil and interface). In other words, matric suction along the shearing plane is approximately constant prior to the peak shear strength. The matric suction corresponding to different initial water content values can be estimated from the measured SWCC shown in Fig. 1. However, as the shearing process continues, soil matric suction gradually reduces due to changes that arise in soil water menisci induced by increment in shear displacement and likely volume changes associated with dilations or contractions. Finally, the soil water menisci completely rupture and there will be negligible or no contribution from matric suction to the post-peak interface shear strength (Hamid and Miller 2009; Houry et al. 2010). The determined or calculated soil and interface shear strength parameters using Eq. (1) to Eq. (4) are summarized in Table 2.

## 2.2. Pile infiltration test (PIT)

In geotechnical engineering practice, it is recommended to locate the pile base on rock or rigid soil layers to provide adequate end bearing capacity. However, in several scenarios expansive soil layers are thick; due to this reason, it may be not always possible to have the pile end on a favorable bearing stratum in expansive soils. Nelson et al. 2012, suggested such piles behavior is similar to that of floating piles. In other words, floating piles support the loads along their length (i.e. shaft friction). For such a scenario, the shaft resistance has to be determined taking account of the influence of both suction changes and volume change behavior of expansive soil around the pile. In the present study, the PIT test has been specially designed to investigate the floating pile behavior taking account of both suction and volume changes of expansive soils on the pile.

The model PIT performed in Regina clay in this study satisfies the following three key criteria. Firstly, the PIT well simulates the commonly encountered in-situ scenario in which infiltration happens during the service stage of the pile. Secondly, all the data required for the rational interpretation of the pile load transfer mechanism were col-

Table 2  
 Soil and interface shear strength parameters of Regina clay.

Internal friction angle with respect to net normal stress ( $I'$ )	15.6°
Internal friction angle with respect to matric suction ( $I_b$ )	12.3°
Interface friction angle with respect to net normal stress ( $d'$ )	12.4°
Interface friction angle with respect to matric suction ( $d_b$ )	8.5°

lected. Thirdly, influence of suction was investigated for rational interpretation of the load transfer mechanism variations.

The PIT was conducted in a cylindrical aluminum tank with an internal diameter of 300 mm and a height of 700 mm following a three-step-procedure as described in Fig. 2 [(A) to (C)]. The model pile is made of an aluminum pile which has an outer diameter of 25.4 mm, a wall thickness of 3 mm and a height of 600 mm. In the first step [Fig. 2(A)], the prefabricated model pile, which was made by pasting a thin fine sand layer to an aluminum pipe, was fixed to the loading machine using a bolt to keep its position fixed during the compaction process. A water-proof ruler was pasted on the inner wall of the aluminum testing tank. The soil displacement during compaction, loading and infiltration process was measured and recorded with the assistance of image technique by continuously taking photos using a digital camera. The ratio of the diameter of testing tank to the diameter of the model pile was designed to be around 12, which is considered satisfactory to alleviate the influence of boundary effects on the PIT results on unsaturated soils (Fan 2007; Han et al. 2016).

In the second step [Fig. 2(B)], fine sand was poured into the testing tank to achieve 150 mm height. A floating model pile with a load cell at bottom were placed on the sand layer. After following these initial precautions, the soil that was already mixed with a water content of 27% was compacted in 20 equal layers (each layer with a thickness of 20 mm) to achieve a wet density of  $1736 \text{ kg/m}^3$  (i.e. dry density of  $1367 \text{ kg/m}^3$ ). In other words, the length of the model pile buried inside expansive soil is 400 mm. During the compaction process of various soil layers, GS-3 and MPS-6 sensors were placed at various positions as shown in Fig. 2(B), for volumetric water content and suction measurements, respectively. Table 3 summarizes the key details of various sensors used for collecting data during the PIT. In the third step [as shown in Fig. 2(C)], the loading machine that was used to keep the pile in a fixed position was removed and the load tank was connected to the pile head. This tank facilitates to add load using lead shots. Two dial gauges were set at the top of the load tank to record the pile displacement during the loading and infiltration process. The bearing capacity of the model pile was estimated to be around 1000 N using Eq. (5) from Chinese Technical Code for Building Pile Foundations (JGJ94–2008). Using a factor of safety of two, a service load of 500 N was applied on the pile head prior to water infiltration. After reaching a stable pile displacement, which was typically observed within 24 h, water was added manually, as and when required, to assure the ground water table was always higher than the ground surface. The soil deformation was measured along with the pile mechanical behavior which include the pile head displacement, pile axial force and

pile base resistance during the period of manual irrigation. Experiment was terminated when the pile head displacement stabilized and all the MPS-6 sensors

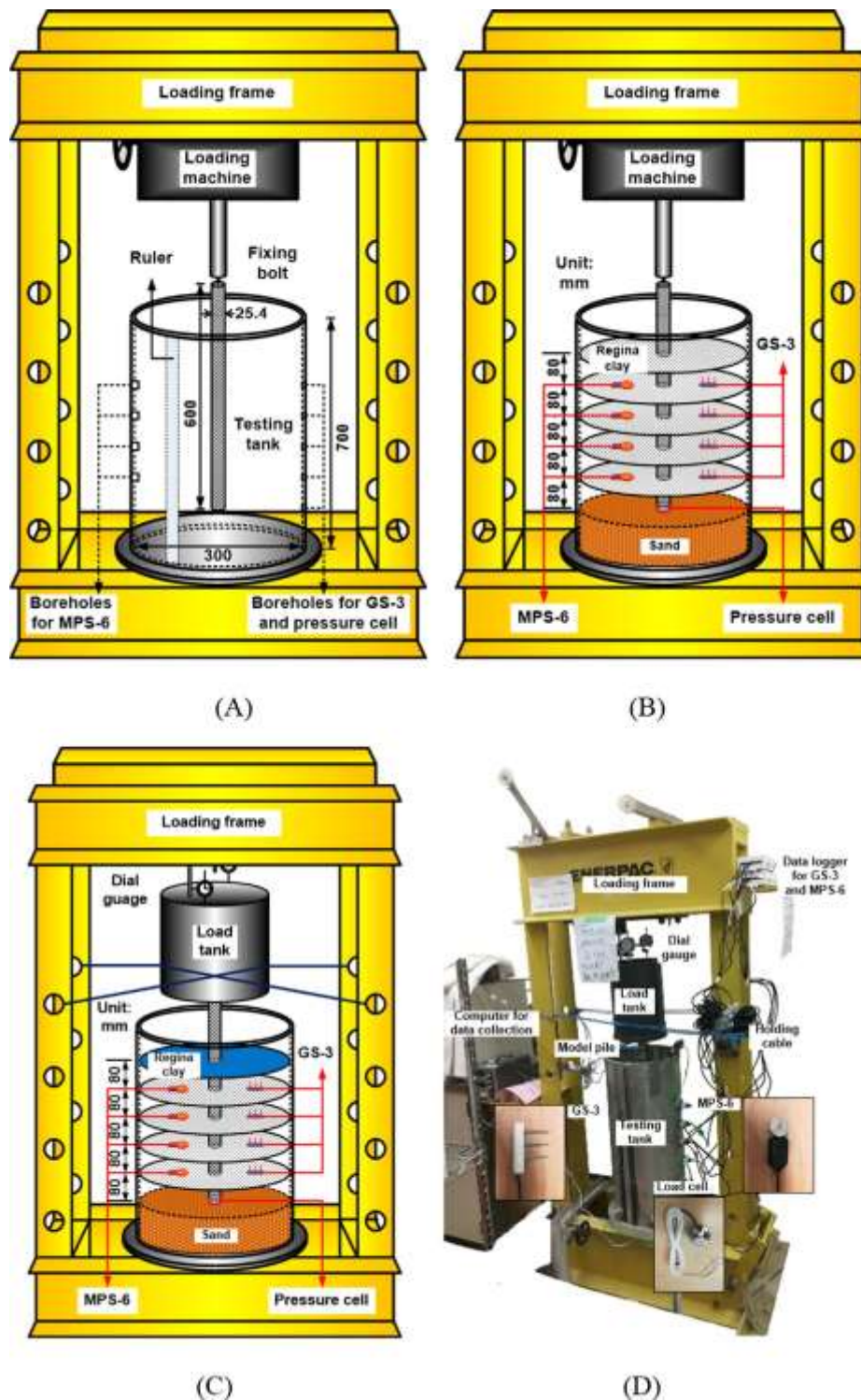


Fig. 2. Three step procedure for conducting the pile infiltration test in expansive soils (A) Step 1; (B) Step 2; (C) Step 3; (D) Equipment set-up photograph.

indicated that the soil has been fully saturated. Fig. 2(D) provides a photographic view of experimental settings during the infiltration stage.

where  $Q_{uk}$  is the ultimate single pile bearing capacity;  $Q_{us}$  is the ultimate pile shaft resistance;  $Q_{pk}$  is the ultimate pile base resistance;  $u$  is the perimeter of the model pile;  $q_{sik}$  is the standard pile shaft friction within soil layer  $i$ , for pre-cast concrete pile with pile shaft in contact with high plas-

Table 3  
Various sensors used in the experimental program along with their details.

Sensor	Manufacturer	Range	Resolution	Accuracy
GS-3 water content sensor	Decagon Devices, Inc.	Apparent dielectric permittivity: 1 (air) to 80 (water)	(0.2% VWC) from 0 to 40% VWC; (0.1% VWC) > 40% VWC.	±3% VWC
MPS-6 dielectric water potential sensor	Decagon Devices, Inc.	—9 to —100000 kPa	0.1 kPa	± (10% of reading + 2 kPa)

stress, for pre-cast concrete pile with pile base on loose fine sand, the  $q_{pk}$  is estimated as 500 kPa;  $A_p$  is the pile base area.

### 2.3. Experimental results

The PIT was performed after the pile settlement stabilized which was 3 mm under the applied the static pile load of 500 N. The PIT required around 40 h for the soil around the pile to fully saturate the expansive soil layer with a thickness of 400 mm. Fig. 3 shows the variations of the soil and pile head displacement upon water infiltration. As water was added manually, soil around the pile experienced volume expansion in the vertical direction, which is consistent with the ground heave. Within 40 h, which was the time required for the expansive soil layer to saturate, the ground heave increased from zero to approximately 25 mm and the pile head settlement increased from 3 mm to around 7 mm. It should be noted that the soil volume increases significantly during the infiltration process with suction reductions, which contributes to an increase in the coefficient of permeability. This is the main reason responsible for the saturation of the soil around the pile in a short time (i.e. 40 h). Also, the shape of SWCC changes due to the volume expansion of expansive soil,. However, considering the difficulty and complexity involved in analyzing the SWCC of expansive soil under

different stress and matric suction conditions, in the present study the influences of volume changes on the SWCC are neglected. Expansive soil collected from the top surface after the infiltration test was close to slurry. Fig. 4(A) and (B), respectively summarize the volumetric water content and the suction changes during the testing period; the pore air pressure was assumed to be zero.

Fig. 5(A) shows the pile axial force variations recorded by strain gauges installed at different depth levels along the model pile. Results summarized in this figure suggest that the pile axial force was continuously increasing during the infiltration process. In addition, these results suggest pile axial force increment was more significant at a greater depth. Fig. 5(B) shows the variations of the pile base resistance during the testing process. During the static loading process, the pile base resistance gradually stabilized at a value of 34 N, which indicated that the upper load was mainly borne by shaft friction and the pile behaves similar to a floating pile. However, during the infiltration process, the pile base resistance grew rapidly to a value of around 183 N, within 40 h. The results suggests that more pile head load was transferred to the pile base. In other words, the pile shaft friction reduced during the infiltration process. The slight increment in the pile base resistance after infiltration for 40 h can be attributed to the relaxation of soil stress, as the expansive soil has been saturated.

### 3. Analysis on experiment results using PEI

#### 3.1. Computation program PEI

The PEI (Pile behavior in Expansive soil upon Infiltration) program developed by Liu and Vanapalli (2019a) was used to interpret the experimental results of the PITs undertaken in present study. The program PEI introduces suction-dependent load transfer curve models and suction-dependent pile-soil relative displacement calculations into traditional load transfer method to extend its application to piles in unsaturated expansive soils. The required information for application of PEI includes the suction profile, SWCC and conventional soil properties (i.e. saturated elastic modulus, Poisson's ratio, soil and interface shear strength properties and vertical swelling pressure of expansive soil), which are either presented in the experimental (positive displacement indicates upward displacement and negative value indicates downward displacement).

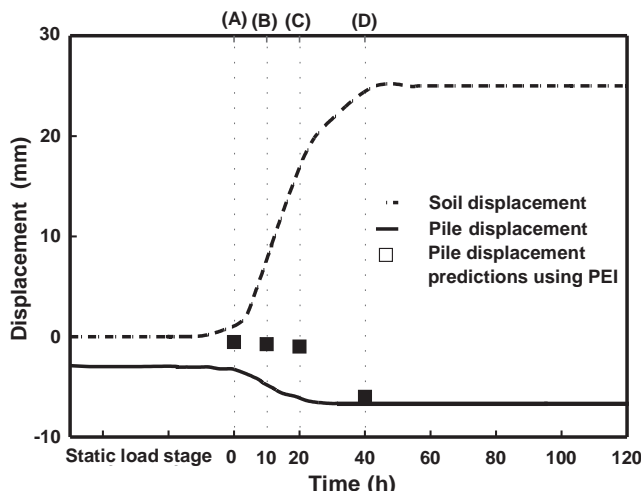


Fig. 3. Variation of soil and pile head displacement with respect to time

results or summarized in [Table 4](#). It should be noted that the program PEI is developed based on simplified assumptions which assumes the soil element around the pile to be

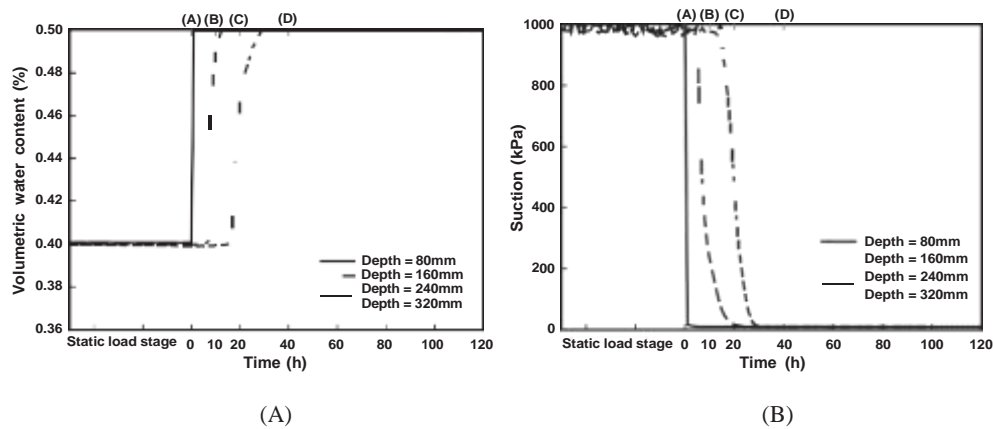


Fig. 4. Variation of (A) volumetric water content and (B) suction distribution with respect to time.

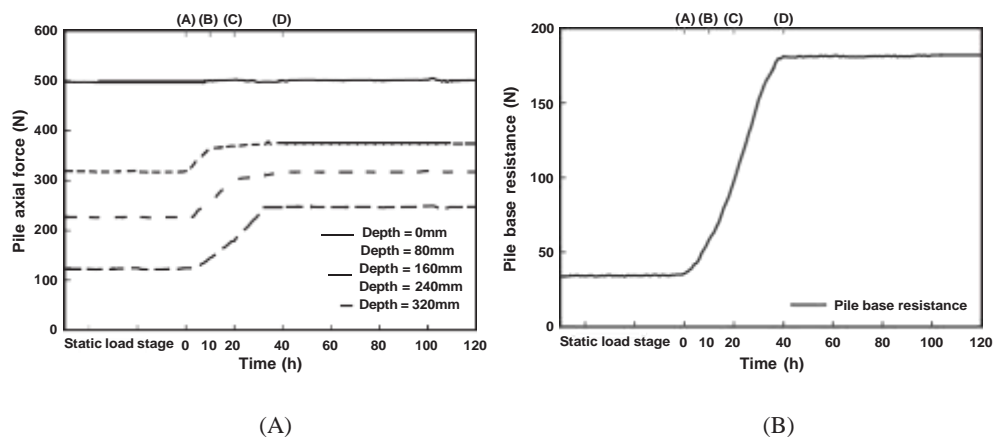


Fig. 5. Variation of pile mechanical behaviors before and after infiltration (A): Pile axial force; (B): Pile base resistance.

Table 4

Various parameters necessary for the application of PEI.

Elastic modulus of saturated Regina clay (kPa)	12,500
Poisson's ratio of Regina clay (Adem and Vanapalli 2016)	0.4
Elastic modulus of the aluminum model pile (GPa)	69
Elastic modulus of sand below the model pile (kPa)	1000
Critical pile-soil relative displacement corresponding to the peak interface shear strength (m) (Zhang et al. 2010, 2011a and 2011b)	0.01
Ratio of residual interface shear strength to peak interface shear strength (Zhang and Zhang 2012)	0.85

isotropic, homogeneous and elastic in nature without any plastic deformation (such as collapse of soil structures due to over-load) during the swelling process (Terzaghi 1925, 1926; 1931). While clay soils can only develop stable structures and constant material properties after repeated wet/dry cycles associated with environmental factors (Kodikara et al. 2002), and typically behave in an elastic manner (Gould et al. 2011; Kodikara 2012). In other words, expansive soil basically exhibits elastic-plastic behaviors during volume expansion. The sand that was poured into the testing tank below the floating pile used in the experimental set up was in a relatively loose state. The elastic modulus of the loose sand is estimated to be around 1000 kPa according to the relationship between pile base resistance and settlement using the PEI as illustrated

in Liu and Vanapalli (2019).

*3.2. Theoretical analysis on pile load transfer mechanism variations*

The pile mechanical behavior at four different time periods of the infiltration process (i.e. 0 h, 10 h, 20 h and 40 h) were selected for interpreting the pile load transfer mechanism changes. These four time points were selected since suction profiles as recorded by buried sensors provide a comprehensive information of the suction variations during the infiltration process (as shown in Fig. 4). Fig. 6 and Fig. 3 shows the comparisons between experimental data and simulations by PEI on pile axial force distributions and pile head displacement, respectively. There is a good agreement achieved between the program PEI simulations and the experimental results of the PIT. These results suggest that

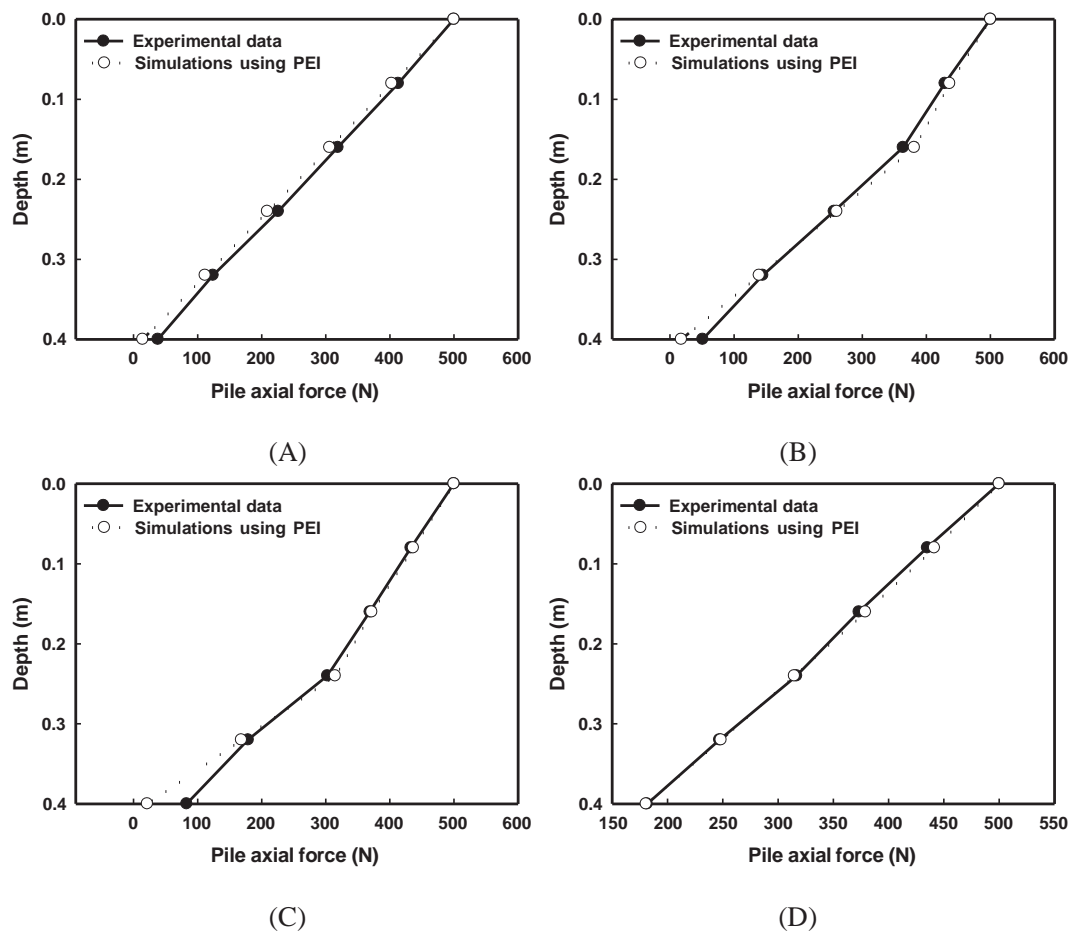


Fig. 6. Comparisons of the pile axial force distribution between experiment data and simulations using PEI [(A) 0 h; (B) 10 h; (C) 20 h; (D) 40 h].

PEI can be used as tool to model and investigate the pile behaviors.

Experimental results regarding the pile mechanical behavior (see Fig. 3 and Fig. 5) indicate that during the infiltration process, pile shaft friction gradually decreased in the already saturated zone but increased within the unsaturated zone. Such a behavior can be attributed to gradual pile head load transfer to the lower part of the pile and pile base. In other words, it is the pile shaft friction variation that has contributed to pile load transfer mechanism changes. With the aid of PEI, the influence of suction and its variations on the shaft friction mobilization can be analyzed comprehensively.

Information related to the pile shaft friction mobilization is determined considering three key factors; namely, net normal stress, suction acting on the pile shaft and pile-soil relative displacement. Figs. 7, 8 and 9 that were developed with the assistance of PEI, summarize the variations of suction, lateral earth pressure (net normal stress) and pile-soil relative displacement variations during the infiltration process, respectively. As shown in Fig. 7, suction gradually decreased from an initial value of 1000 kPa to zero with the depth as the saturation process

continued. At the same time, suction reduction triggered

the mobilization of lateral swelling pressure which contributed to an additional increment to the lateral earth pressure due to soil self-weight. As a consequence, lateral earth pressure gradually increased from top to the bottom of the pile (as shown in Fig. 8). Fig. 9 shows that the pile-soil relative displacement gained significant increment with the development of ground heave. Also, the increasing pile-soil relative displacement showed a linear distribution from the wetting depth to the ground surface. The pile-soil relative displacement at the upper part of the pile has exceeded the critical value when the soil in the tank fully saturated; such a behavior suggests that the pile shaft friction at this stage reaches a residual value.

In the computation program PEI, the interface shear strength is calculated using Eq. (4) proposed by Hamid and Miller (2009). In this equation, the first two terms indicate the contribution of net normal stress and true cohesion to the pile shaft friction while the last term indicates the contribution of matric suction to the pile shaft friction. Using the information provided in Fig. 7 to Fig. 9, it is possible to separately consider the contributions of net normal stress and matric suction to the pile shaft friction. More specifically, according to the net normal stress distribution as shown in Fig. 8 and pile-soil interface shear strength

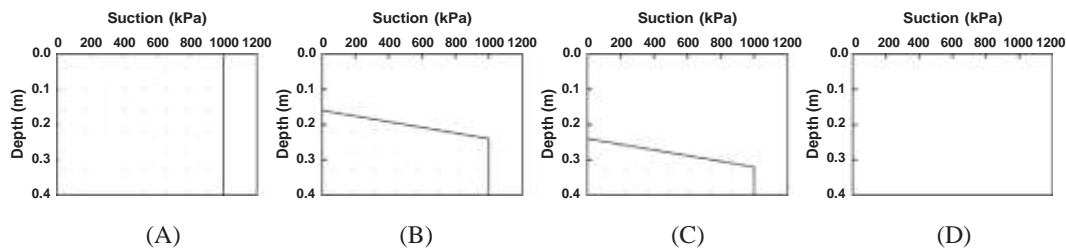


Fig. 7. Suction profile at four representative time points [(A) 0 h; (B) 10 h; (C) 20 h; (D) 40 h].

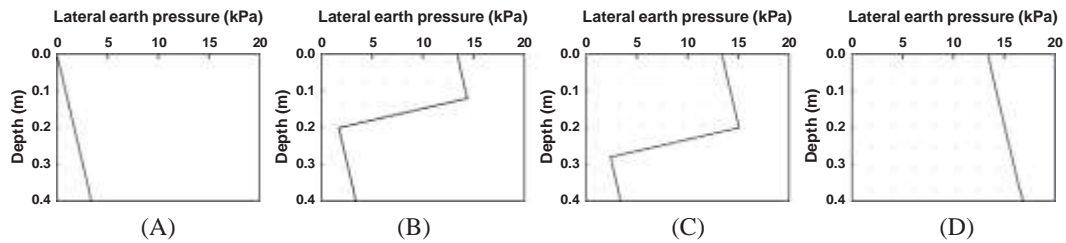


Fig. 8. Lateral earth pressure considering the mobilization of lateral swelling pressure at four representing time points [(A) 0 h; (B) 10 h; (C) 20 h; (D) 40 h].

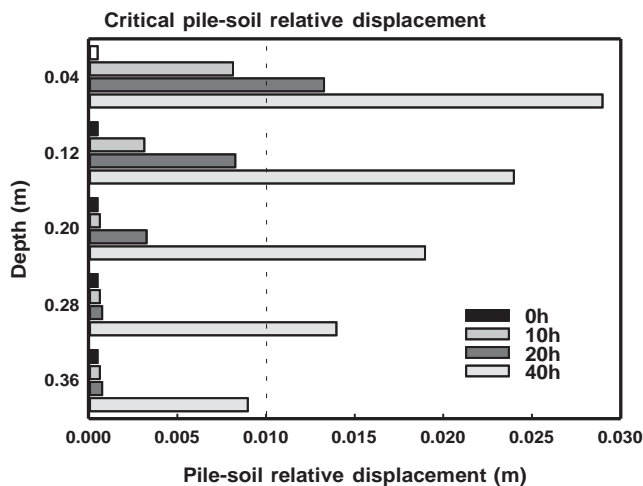


Fig. 9. Pile-soil relative displacement at different time points.

parameters, it is possible to establish the load transfer curve which only considers the contributions of net normal stress and true cohesion to the pile shaft friction. The contribution of net normal stress towards pile shaft friction at a certain time point can be estimated from the pile-soil relative displacement shown in Fig. 9. The contribution of matric suction towards the pile shaft friction is just the difference between the total pile shaft friction and the pile shaft friction associated with net normal stress, as shown in Fig. 10. However, it should be noted that Fig. 10 is presented based on superposition method, which is only capable of providing details of the contributions of net normal stress and matric suction to the pile shaft friction. The net normal stress contributes to the pile shaft friction through soil particle friction while the suction contributes to the pile shaft friction through tension of soil water

Fig. 10. Firstly, the peak pile shaft friction under saturated state was lower in comparison to unsaturated state. Secondly, the contribution of suction to pile shaft friction decreased while the contribution of net normal stress to pile shaft friction increased during the infiltration process. The total pile shaft friction decreased as infiltration continued, since the reduction in pile shaft friction due to suction reduction was predominant.

Fig. 11 (A) to (E) which were generated using PEI, clearly demonstrate that during infiltration process (from 0 to 40 h), the load transfer curve shape varies significantly at different levels of depth (from 0.04 m to 0.36 m) and influences of pile-soil relative displacement increment on the pile shaft friction mobilization. The load transfer curve menisci. Two general observations can be derived from

variations indicate both peak and post-peak pile shaft friction reduce from an unsaturated to a saturated state. Also, at the same depth, the pile-soil relative displacement keeps increasing during the infiltration process due to pile settlement increment and ground heave development. According to Fig. 11, prior to water infiltration under the applied static load, pile-soil relative displacement has not reached the critical value [see Fig. 11 (A) to (E)]. There is pile shaft friction loss in the already saturated zone due to the influence of water infiltration. However, the pile shaft friction in unsaturated zone increased to a peak value due to pile-soil relative displacement increment [see Fig. 11 (C) to (E)]. On the contrary, significant pile-soil relative displacement increment contributed to pile-soil interface shear strength reduction from peak to a post-peak value in the already saturated zone [see Fig. 11 (A) to (B)].

### *3.3. Theoretical model for the estimation of threshold load*

The PIT conducted in present study showed that pile shaft friction under the service load calculated using Eq.

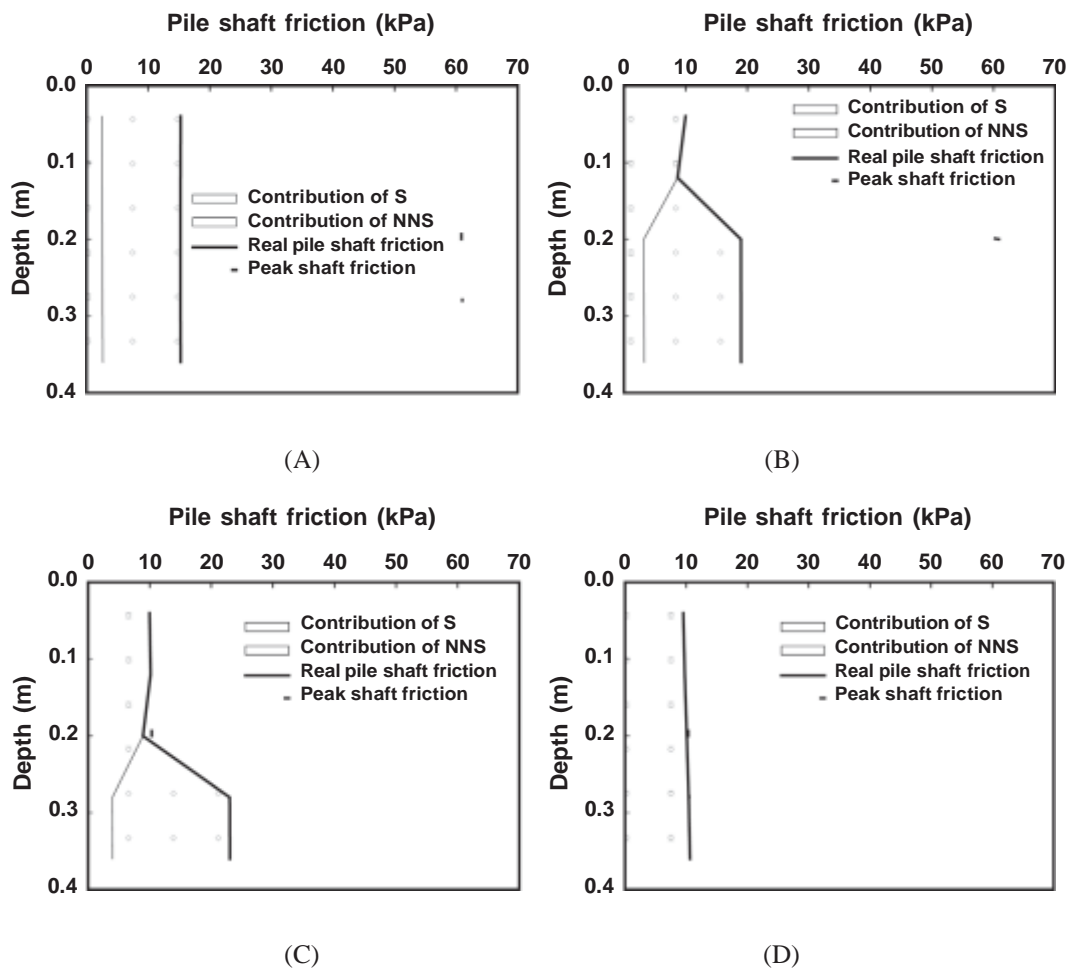


Fig. 10. Contributions of net normal stress (NNS) and matric suction (S) to the pile shaft friction at four representing time points [(A) 0 h; (B) 10 h; (C) 20 h; (D) 40 h].

(5), reduced due to water infiltration. Such a behavior can be attributed to significant pile head load transfer to pile base resulting in a further pile head settlement. Similar trends of results were reported from the centrifuge test conducted by Yang et al. (2017). However, it is of interest to note that, there are several PITs reported in literature in which uplift displacement was observed in the pile, if there was no pile head load (for example, Mendoza 2013; Fan et al. 2007; Al-Rawas and Goosen 2006; Benvenga 2005). These observations suggest that there should be a certain pile head load for pile settlement to occur upon water infiltration. In the present study, this value of pile head load is referred to as the threshold load. A floating pile that supports a light structure on which pile head load is lower than the threshold load is likely to undergo uplift displacement. For such a scenario, the influence of uplift friction should be accounted for in the design of piles. However, when pile head loads are higher than the threshold value, various safety and stability problems associated with the further settlement of the pile should be considered.

For piles in unsaturated expansive soils, it is the pile

shaft friction variations in the active zone which predominantly influences the pile load transfer mechanisms prior to

and after water infiltration. As shown in Fig. 12(A), the pile shaft friction shows a rectangular distribution in the active zone assuming pile-soil relative displacements along the entire pile are the same due to the high stiffness of pile. As water infiltrates into soil around the pile, both the shape of the load transfer curve and pile-soil relative displacement change. If there is no pile head displacement, the resultant of the pile shaft friction within the active zone should be the same prior to and after water infiltration (i.e. independent of degree of the saturation). Such a scenario is shown in Fig. 12(B). After saturation, reduction in both peak interface shear strength and residual shear strength results in load transfer curve changes. Although the pile shaft friction shows a curve-shaped distribution due to pile-soil relative displacement increment, the area of the pile shaft friction distribution ( $S_2$ ) is equivalent to the pile shaft friction resultant ( $S_1$ ), which represents the resultant of pile shaft friction before saturation. For such scenarios, the load applied on the pile head is the threshold pile head load. In PEI, the shape of the load transfer curve is described by Eq. (6), thus the area of  $S_1$  and  $S_2$  equivalent to the resultant can be deduced as Eq. (8) and (9), respectively.

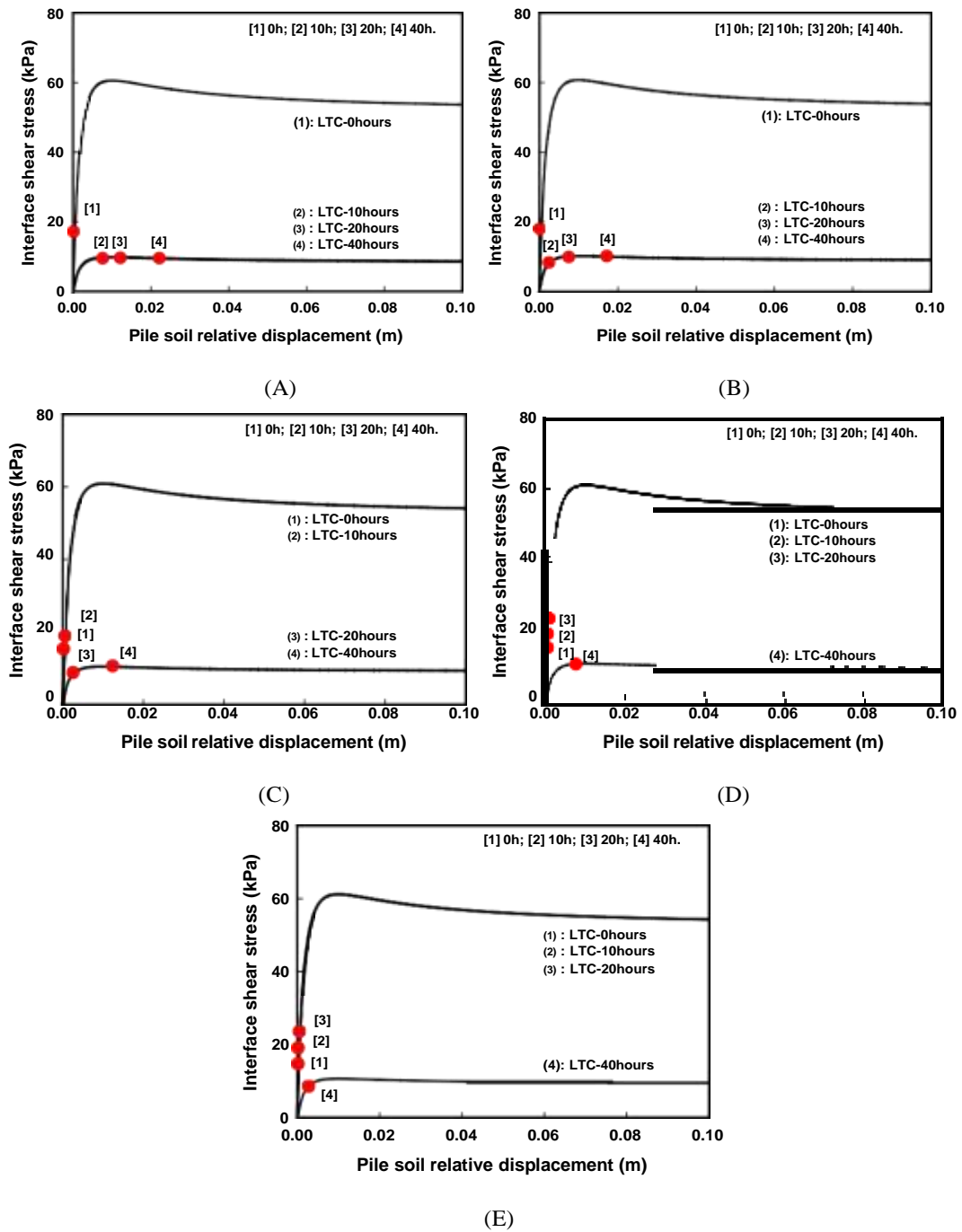


Fig. 11. Pile shaft friction (PSF) variations at different depths [(A) 0.04 m; (B) 0.12 m; (C) 0.2 m; (D) 0.28 m; (E) 0.36 m] in the infiltration process illustrated using load transfer curve (LTC).

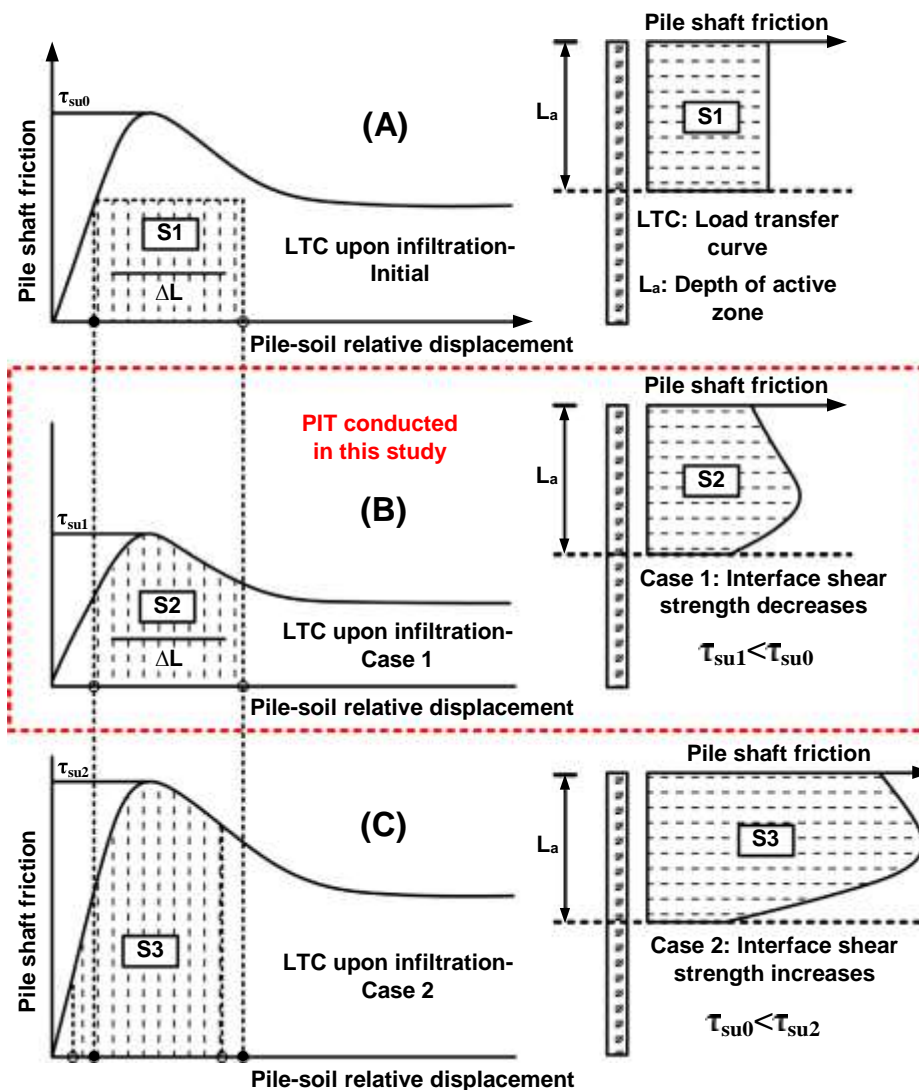


Fig. 12. Load transfer curves and pile shaft friction distribution patterns before and after saturation.

where  $Dh_s$  is the total ground heave developed from initial unsaturated condition to a fully saturation, which can be calculated using Eq. (14) proposed by Adem and Vanapalli (2016).

where  $Dh_s$  is the total ground heave of soil;  $D(u_a - u_w)$  is the matric suction reduction.

The only unknown parameter  $S_{s(i)}$  can be solved using numerical methods by combining Eqs. (12) and (13). Once  $S_{s(i)}$  value is solved, the threshold pile head load  $Q_{ref}$  can be determined using Eq. (15). For the PIT presented in this study, after water infiltration, the pile shaft friction in the active zone decreases since the pile shaft friction reduction due to suction reduction is more significant than the pile

soil relative displacement difference ( $DL$ ) can be estimated using Eq. (13) and (14) based on the depth of the active zone and some basic soil properties. The threshold pile head load can be estimated using Eq. (15) from soil and interface properties and site investigations studies which assist in the determination of depth of active zone.

#### 4. Summary and conclusions

shaft friction increment due to lateral swelling pressure mobilization. Therefore, as illustrated in Fig. 12(B), there exists a threshold load which distinguishes whether the pile would experience uplift displacement or further settlement upon water infiltration. The threshold load is estimated to be around 326 N using Eq. (15), which needs only basic soil properties. This result is also consistent with the value acquired through PEI. The applied pile head load 500 N is higher than the threshold load, as a consequence, pile has

changes associated with water infiltration. In the present study, water infiltration test was conducted in a laboratory environment to investigate the behavior of a model floating pile in an expansive soil, taking account of the influence of stress and hydraulic boundary conditions that are typically encountered in practice. Experimental results were analyzed using a computation program PEI (i.e. Pile behavior in Expansive soil upon Infiltration) developed by [Liu and Vanapalli \(2019a\)](#) which highlights the influence of suction and suction variations induced volume changes of expansive soils on the load transfer mechanism of the model pile. Following conclusions can be summarized from the investigations undertaken in this study.

- (1) The pile shaft friction mobilization and the pile load transfer mechanisms are combined influenced by the variations in the net normal stress, suction and pile-soil relative displacement. For a pile in expansive soil with a service load, water infiltration causes a reduction in the pile shaft friction within the active zone for two reasons. Firstly, the pile shaft friction reduction due to suction reduction in the active zone is more predominant than the pile shaft friction increment associated with the mobilization of lateral swelling pressure. Secondly, the pile-soil relative displacement increment increases the pile-soil interface shear strength (shaft friction) towards the peak value at greater depth but reduces pile-soil interface shear strength at shallow depth from the peak value to post-peak value. Therefore, more pile head load is gradually transferred to the pile at a greater depth, resulting in the increment of the pile base resistance and pile head settlement.
- (2) Floating piles in expansive soil may either undergo uplift displacement or further settlement under the influence of water intrusion predominantly in the active zone. The pile typically experiences uplift displacement due to generation of uplift friction for cases in which the pile shaft friction increases after water infiltration due to mobilization of lateral swelling pressure. While for the cases in which the pile shaft friction reduces after water infiltration due to suction reduction, there exists a threshold pile head load under which the pile head displacement remains unchanged prior to and after water infiltration. If the pile head load is lower than this threshold value, the pile undergoes uplift displacement with an increase in the degree of saturation and after the soil reaches saturated condition. On the contrary, a higher pile head load results in a pile settlement after the soil reaches fully saturation condition.
- (3) A theoretical model is proposed for the estimation of threshold pile head load using unsaturated soil mechanics principles. The proposed model is simple

and requires only basic soil properties, interface shear strength properties and depth of active zone for use in geotechnical engineering practice. The proposed model is valuable for practicing engineers to make quick and reasonable evaluations of pile mechanical behaviors variations in unsaturated expansive soils during the water infiltration process. In other words, the studies provide valuable information for rational pile foundations designs taking account of influence of environmental factors

Kodikara, J., 2012. New framework for volumetric constitutive behaviour of compacted unsaturated soils. *Can. Geotech. J.* 49 (11), 1227–1243.  
Liu, Y., Vanapalli, S.K., 2017. Influence of lateral swelling pressure on the geotechnical infrastructure in expansive soils. *J. Geotech. Geoenviron. Eng.* 04017006.

## References

- Adem, H.H., Vanapalli, S.K., 2016. Heave prediction in a natural unsaturated expansive soil deposit under a lightly loaded structure. *Geotech. Geolo. Eng.* 34 (4), 1181–1192.
- Al-Rawas, A. A., Goosen, M. F. A., 2006. Expansive soils, recent advances in characterization and treatment. *Bulletin of Engineering Geology and the Environment.* 66(4), 505-505.
- Benvenega, M.M., 2005. Pier-soil adhesion factor for drilled shaft piers in expansive soil M.S. thesis. Colorado State University, Colorado, USA.
- Elsharief, A.M., 1987. Foundation on expansive soils: A laboratory and field investigation of Swelling Potential and Performance of Short piles in Expansive soils M.S Thesis. University of Khartoum, Building and Road Research Institute, Sudan.
- Fan, Z.H., Wang, Y.H., Xiao, H.B., Zhang, C.S., 2007. Analytical method of load-transfer of single pile under expansive soil swelling. *Journal of Central South University of Technology.* 14 (4), 575–579.
- Fan, Z.H., 2007. Research on swelling-shrinkage characteristic and pile-soil interaction of expansive soil foundation PhD thesis. Central South University, Changsha, China. (In Chinese).
- Fredlund, D.G., Morgenstern, N.R., Widger, R.A., 1978. The shear strength of unsaturated soils. *Can. Geotech. J.* 15 (3), 313–321.
- Fredlund, D.G., Xing, A., 1994. Equations for the soil-water characteristic curve. *Can. Geotech. J.* 31 (4), 521–532.
- Fredlund, D.G., 2019. State of Practice for use of the Soil-Water Characteristic Curve in Geotechnical Engineering. *Can. Geotech. J.* 56 (8), 1059–1069.
- Gould, S.J., Kodikara, J., Rajeev, P., Zhao, X.L., Burn, S., 2011. A void ratio–water content–net stress model for environmentally stabilized expansive soils. *Can. Geotech. J.* 48 (6), 867–877.
- Hamid, T.B., Miller, G.A., 2009. Shear strength of unsaturated soil interfaces. *Can. Geotech. J.* 46 (5), 595–606.
- Han, Z., Vanapalli, S.K., Kutlu, Z.N., 2016. Modeling behavior of friction pile in compacted glacial till. *Int. J. Geomech.* 16 (6), D4016009.
- IS: 2720 (Part XL)-(1977). Methods of Test for Soils: Part-XL. Determination of free swell index of soil, Bureau of Indian Standards, New Delhi.
- Jaremski, J., 2012. Application of the joining pile for foundations on expansive clays and rocks. *American International Journal of Contemporary Research.* 2 (10), 53–58.
- Jiang, G., Chen, W., Liu, X., Yuan, S., Wu, L., Zhang, C., 2018. Field study on swelling-shrinkage response of an expansive soil foundation under high-speed railway embankment loads. *Soils Found.* 58 (6), 1538–1552.
- Jain, A.K., Jha, A.K., 2020. Geotechnical behaviour and micro-analyses of expansive soil amended with marble dust. *Soils Found.* 60 (4), 737–751.
- Khoury, C. N., Miller, G. A., Hatami, K., 2010. Shear strength of unsaturated soil-geotextile interfaces. *GeoFlorida 2010, Advances in Analysis, Modeling and Design.* 307-316.
- Kodikara, J., Barbour, S., Fredlund, D.G., 2002. Structure development in surficial heavy clay soils: a synthesis of mechanisms. *Australian Geomechanics: Journal and News of the Australian Geomechanics Society* 37 (3), 25.

- Liu, Y., Vanapalli, S.K., 2019a. Load displacement analysis of a single pile in unsaturated expansive soil upon water infiltration. *Comput. Geotech.* 106, 83–98.
- Liu, Y., Vanapalli, S.K., 2019b. Mobilization of lateral swelling pressure of expansive soil in the lab and field. *Soils Found.* 59 (1), 176–195.
- Lu, N., 2008. Is matric suction a stress variable? *J. Geotech. Geoenviron. Eng.* 134 (7), 899–905.
- Mendoza, C., 2013. Measurement of friction on piles over neutral plane in expansive soils. *Advances in unsaturated soils-Caicedo et al. (eds), 2013 Taylor & Francis Group, London.* 592.
- Mohamedzein, Y.E.A., Mohamed, M.G., Sharief, A.M.E., 1999. Finite element analysis of short piles in expansive soils. *Comput. Geotech.* 24 (3), 231–243.
- Nelson, J.D., Thompson, E.G., Schaut, R.W., Chao, K.C., Dunham-Friel, J.S., 2012. Design procedure and considerations for piers in expansive soils. *J. Geotech. Geoenviron. Eng.* 138 (8), 945–956.
- Nur Eldayem, F.E., 1999. Effect of Interface on Soil Pile Interaction in Expansive Soil. University of Khartoum, Sudan.
- Oloo, S.Y., Fredlund, D.G., 1996. A method for determination of FB for statically compacted soils. *Can. Geotech. J.* 33 (2), 272–280.
- Osman, M.A., Charlie, W.A., 1983. *Expansive Soils in Sudan. BRRI Current Paper CP 3/83.* University of Khartoum, Sudan.
- Osman, M., Elsharief, A.M., 1999. Field experiments on piles in the expansive soils of central Sudan. *Build. Road Res. J.* 2, 17–26.
- Phanikumar, B.R., Sharma, R.S., Rao, A.S., Madhav, M.R., 2004. Granular pile anchor foundation system for improving the engineering behaviour of expansive clay beds. *Geotech. Test. J.* 27 (3), 279–287.
- Prakash, C., Ramakrishna, V.V.G.S.T., 2004. Lateral load capacity of under reamed piles: An analytical approach. *Soils Found.* 44 (5), 51–65.
- Poulos, H.G., Davis, E.H., 1980. *Pile Foundation Analysis and Design.* John Wiley & Sons.
- Pham, H.Q., Fredlund, D.G., Barbour, S.L., 2005. A study of hysteresis models for soil-water characteristic curves. *Can. Geotech. J.* 42 (6), 1548–1568.
- Soundara, B., Robinson, R.G., 2017. Hyperbolic model to evaluate uplift force on pile in expansive soils. *KSCE J. Civ. Eng.* 21 (3), 746–751.
- Sharma, R.S., Phanikumar, B.R., 2005. Laboratory study of heave behavior of expansive clay reinforced with geopiles. *J. Geotech. Geoenviron. Eng.* 131 (4), 512–520.
- Sheng, D., Yamamoto, H., Wriggers, P., 2008. Finite element analysis of enlarged end piles using frictional contact. *Soils Found.* 48 (1), 1–14.
- Terzaghi, K., 1925. *Principles of soil mechanics: I - Phenomena of cohesion of clays.* *Engineering News-Record* 95 (19), 742–746.
- Terzaghi, K. (1926). "The mechanics of adsorption and swelling of gels." 4th Colloid Symposium Monograph, Chem. Catal. Co., New York, 58-78.
- Terzaghi, K. (1931). "The influence of elasticity and permeability on the swelling of two-phase systems." *Colloid Chemistry*, J. Alexander, ed., 3, New York, Chem. Catal. Co., 65-88.
- Vanapalli, S.K., Fredlund, D.G., Pufahl, D.E., Clifton, A.W., 1996. Model for the prediction of shear strength with respect to soil suction. *Can. Geotech. J.* 33 (3), 379–392.
- Wu, W., Song, H.Z., Wang, H.Y., Liu, C.J., Jiang, Y., 2012. Prototype experimental study of expansive force of pile embedded in expansive soil. *Rock and Soil Mechanics.* 33 (2), 173–177.
- Yitagesu, F.A., van der Meer, F., van der Werff, H., Zigterman, W., 2009. Quantifying engineering parameters of expansive soils from their reflectance spectra. *Eng. Geol.* 105 (3–4), 151–160.
- Yang, J., Zhang, D.F., Li, L.Y., Shen, Z.P., 2017. Centrifuge modelling of working performance of foundation pile embedded in expansive clay with high liquid limit. *Chinese J. of Geotech. Eng.* 39 (10), 1770–1776 (In Chinese).
- Zhang, Q.Q., Zhang, Z.M., Yu, F., Liu, J.W., 2010. Field performance of long bored piles within piled rafts. *Proc. Inst. Civ. Eng. Geotech. Eng.* 163 (6), 293–305.
- Zhang, Z.M., Zhang, Q.Q., Yu, F., 2011a. A destructive field study on the behavior of pile under tension and compression. *Journal of Zhejiang University-Science A.* 12 (4), 291–300.
- Zhang, Z.M., Zhang, Q.Q., Zhang, G.X., Shi, M.F., 2011b. Large tonnage tests on super-long piles in soft soil area. *Chinese Journal of Geotechnical Engineering.* 33 (4), 535–543 (In Chinese).
- Zhang, Q.Q., Zhang, Z.M., 2012. A simplified nonlinear approach for single pile settlement analysis. *Can. Geotech. J.* 49, 1256–1266.